

OPEN ACCESS

Formation of microtubes from strained SiGe/Si heterostructures

To cite this article: H Qin *et al* 2005 *New J. Phys.* **7** 241

View the [article online](#) for updates and enhancements.

You may also like

- [p-Type Ion Implantation in Tensile Si/Compressive Si_{0.4}Ge_{0.6}/Tensile Strained Si Heterostructures](#)
R. A. Minamisawa, D. Buca, B. Holländer et al.
- [Boron-Induced Strain Relaxation in Hydrogen-Implanted SiGe/Si Heterostructures](#)
Sheng-Wei Lee, Chi-An Chueh and Hung-Tai Chang
- [Heteroepitaxial growth on thin sheets and bulk material: exploring differences in strain relaxation via low-energy electron microscopy](#)
Chanan Euaruksakul, Michelle M Kelly, Bin Yang et al.

Formation of microtubes from strained SiGe/Si heterostructures

H Qin^{1,4}, N Shaji¹, N E Merrill¹, H S Kim¹, R C Toonen¹,
R H Blick¹, M M Roberts², D E Savage², M G Lagally²
and G Celler³

¹ Laboratory of Molecular-scale Engineering, Department of Electrical and Computer Engineering, University of Wisconsin-Madison, 1415 Engineering Drive, Madison, WI 53706, USA

² Department of Materials Science and Engineering, University of Wisconsin-Madison, 1500 Engineering Drive, Madison, WI 53706, USA

³ SOITEC USA Inc., 2 Centennial Drive, Peabody, MA 01960, USA

E-mail: qin1@wisc.edu

New Journal of Physics 7 (2005) 241

Received 24 June 2005

Published 29 November 2005

Online at <http://www.njp.org/>

doi:10.1088/1367-2630/7/1/241

Abstract. We report the formation of micrometre-sized SiGe/Si tubes by releasing strained SiGe/Si bilayers from substrates in a wet chemical-etching process. In order to explore statistical studies of dynamic formation of microtubes, we fabricated arrays of square bilayers. Due to the dynamic change in curvature of the bilayers, and hence the underlying etch channels, the etching process deviates from a transport-controlled regime to one of kinetic controlled. We identified two distinct modes of etching. A slow etching mode is associated with symmetric surface deformation in which the bilayers mostly retain their initial pattern. In the fast mode, bilayers are asymmetrically deformed while large etch channels are induced and etching becomes kinetically controlled. Etch rate dispersion is directly related to the degree of asymmetry in surface deformation. When the dimensions of the bilayers become significantly larger than the curvature radius, kinetic etching dominates. During the formation of tubes, SiGe/Si bilayers strongly interact with the liquid environment of etchant and solvent. Assisted by the surface tension of evaporating liquids, the tubes are drawn near the substrate and eventually fixed to it because of van der Waals forces. Our study illuminates the dynamic etching and curling processes involved with and provides insight on how a uniform etch rate and consistent curling directions can be maintained.

⁴ Author to whom any correspondence should be addressed.

Contents

1. Introduction	2
2. Experiments	2
3. Results	4
4. Conclusions	8
Acknowledgments	10
References	10

1. Introduction

Three-dimensional micromachining allows one to precisely define and form micrometre-sized devices as components of microelectromechanical systems (MEMS). To take further advantage of the novel functions and miniaturization offered by micromachining, device fabrication is now being pushed towards the nanoscale. Engineering nanoelectromechanical systems (NEMS) has been traditionally focused on applications for radio and microwave frequency sensors and communication electronics [1]–[3]. Nanomechanical resonators have displayed ultra-high sensitivities for charge [4] and displacement detection [5]–[7]. NEMS single-electron transistors (SETs) have operated with frequencies ranging from 1 to 400 MHz at room temperature [8].

Recently, strain initiated from the lattice mismatch in semiconductor heterostructures has been employed to form complex three-dimensional micro/nanostructures [9]–[11]. Combined with conventional optical-/electron-beam lithography, this technique allows one to precisely position, self-assemble and finally release functional nanostructures in a highly controllable manner. Strained silicon-on-insulator (SSOI) is among the materials—the others being SiGe/Si, GaAs/InGaAs and GaAs/InAs—previously used with this technique (for applications of high-speed, low-power consumption and high-density integration) [12, 13]. By combining the high electron mobility in strained silicon and the ability of self-curling, it provides a new approach to make novel MEMS/NEMS devices, such as freely distributed sensors and controlled drug delivery made from microtubes. It is of fundamental importance to study the dynamics of microtube formation, due to the inherent sensitivity to electromagnetic, mechanical forces and surface chemistry. Wet-chemical etching is a critical step in releasing MEMS/NEMS devices, especially, when the devices are subjected to dynamic deformation [14]. In this paper, we study the mechanisms and dynamics involved in self-curling of strained-SiGe/Si heterostructures suspended by under-etching. Arrays of identical squares are patterned to allow a statistical study on the effect of strain-induced surface deformation on the etching of sacrificial layer. When the device dimensions become larger than the curvature radius, a large degree of freedom for the squares to deform themselves disperses the etching process. In order to achieve a well-controlled curling direction and etch rate, both the device pattern and the etchant have to be optimized.

2. Experiments

Arrays of squares were patterned on SiGe/Si bilayer material (prepared by the SOITEC company⁵) using electron-beam lithography, aluminium deposition and lift-off. Reactive-ion etching was used to isolate the bilayer squares from each other. Each array contained 400

⁵ Smart Cut™ are trademark of S O I Tec Silicon on Insulator Technologies (SOITEC, SA).

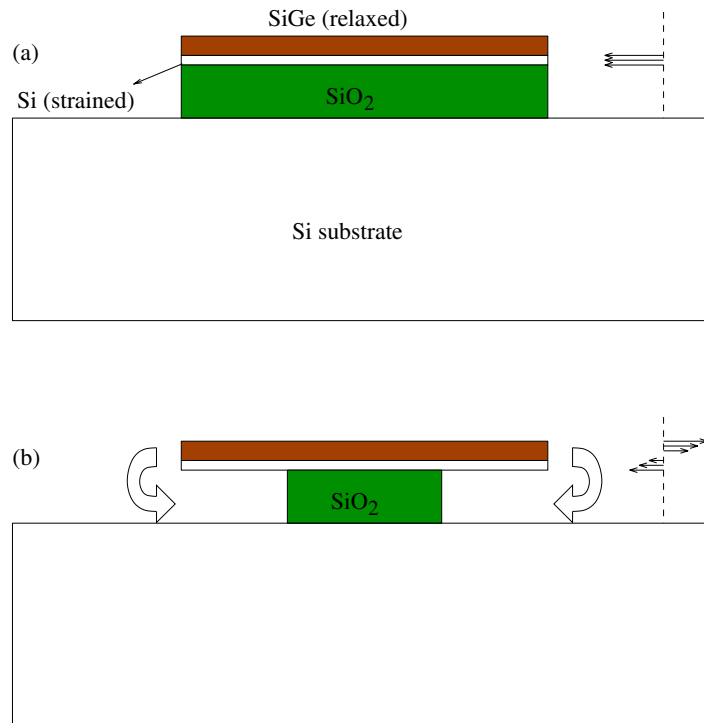


Figure 1. A SiGe/Si heterostructure is released from the substrate by removing the silicon oxide sacrificial layer. The Si layer becomes partly relaxed by transferring part of the strain to the SiGe layer. As a result, the bilayer curves downwards and forms a tube.

squares with identical dimensions allowing for a statistical study of the formation of tubes. As schematically shown in figure 1(a), the bilayer consists of a 50 nm thick layer of relaxed Si_{0.8}Ge_{0.2} over a 20 nm thick layer of strained silicon. The 184 nm thick SiO₂ layer served as a sacrificial layer. This heterostructure was realised using the *Smart Cut* technology (see footnote 5), in which the strained silicon layer was initially grown on relaxed Si_{0.8}Ge_{0.2} and then both layers were transferred to a SiO₂ sacrificial layer on the Si substrate. Both planes of the bilayer and substrate were oriented along crystalline direction (001). Squares were patterned so that the edges were parallel to the $\langle 110 \rangle$ ($\pm 5^\circ$) direction and the diagonals lied along the $\langle 010 \rangle$ ($\pm 5^\circ$) direction. The induced strain from the lattice mismatch between the Si_{0.8}Ge_{0.2} and Si layer was found to be $\epsilon \approx 4.2\% \times x = 8.4 \times 10^{-3}$, where $x = 0.2$ is the Ge fraction in the Si_{0.8}Ge_{0.2} layer and 4.2% is the lattice mismatch between silicon and germanium. To remove the SiO₂ sacrificial layer, hydrofluoric acid buffered by ammonia fluoride (NH₄F : HF = 6 : 1) was used at room temperature. As illustrated in figure 1, once released from the substrate the bilayer curved downward and some of the strain was transferred to the SiGe layer due to the initial compressive strain in the silicon layer. After etching, the samples were transferred into deionized water to remove the etchant. Before the samples were dried in air, acetone and isopropanol rinsing steps were applied. During the transfer of samples from liquid to liquid, special care was taken to prevent suspended tubes from being distributed in liquids. We monitored the etching and tube formation of different sizes of bilayer squares with an optical microscope. The doping level not only affects the electrical properties of the tubes, but also alters the chemical etching

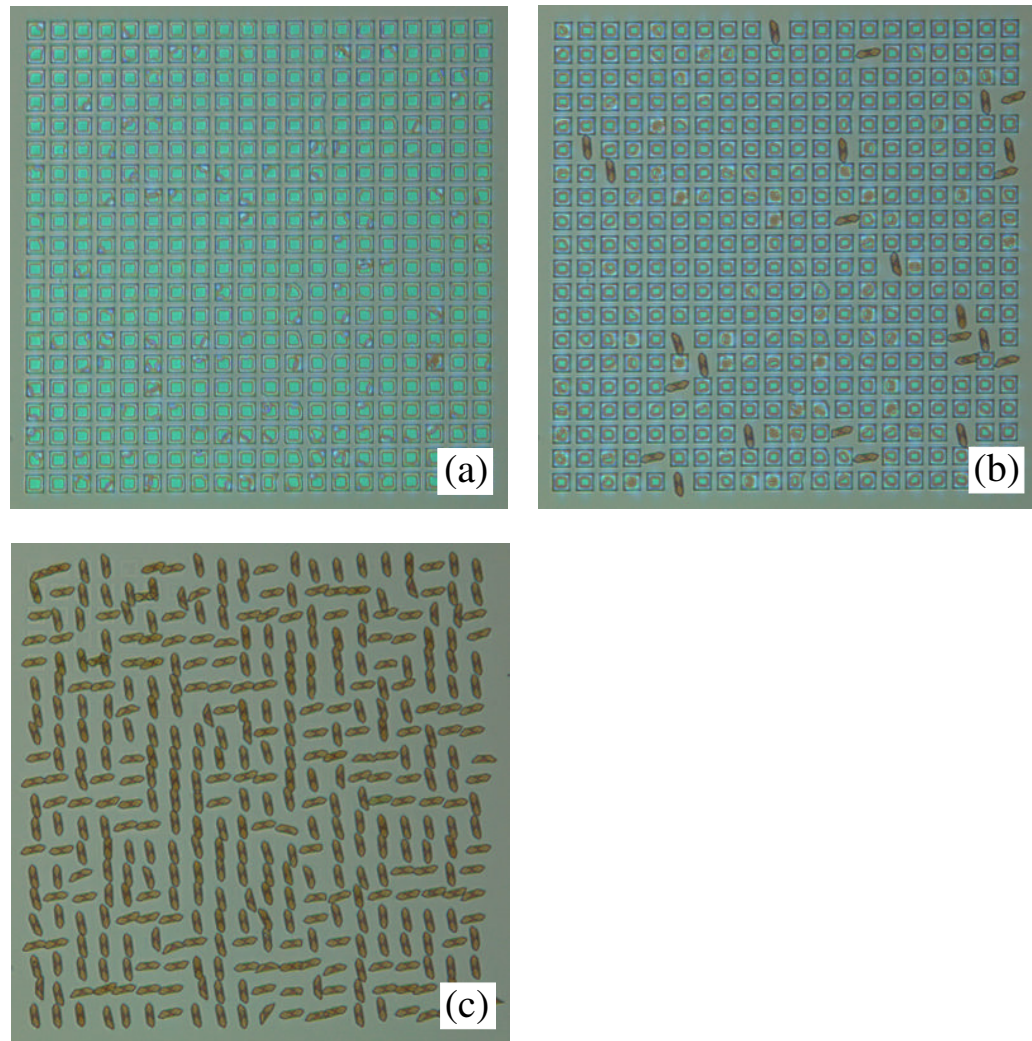


Figure 2. An array of 400 SiGe/Si bilayer squares is etched in a buffered hydrofluoric acid solution for 13.2 min. Snapshots at 20 seconds, 10 min, and 13.2 min are shown in (a), (b), and (c), respectively. Squares have a dimension of $30 \times 30 \mu\text{m}^2$. Squares curve into tubes in the diagonal directions. Formed tubes are orientated at two specific directions ($\leftrightarrow : \updownarrow = 38\% : 62\%$) at right angles with each other. The [video clip](#) shows the complete etching process.

hence the formation of tubes. In this study, the SiGe/Si bilayers were intentionally not doped so as to isolate the mechanisms of dynamic tube formation. Further studies on the formation and electrical manipulation of doped SiGe/Si tubes are currently under investigation.

3. Results

Figure 2 displays three snapshots of an array of $30 \times 30 \mu\text{m}^2$ -sized squares during the etching process (see the caption of figure 2 for a [video clip](#) showing the complete etching process). Since

the relaxed $\text{Si}_{0.8}\text{Ge}_{0.2}$ layer is above the strained Si layer, suspended bilayers curved toward and eventually touched the silicon substrate. Once the downward curling was hindered by the substrate, the etch channels were redirected and reduced in height. However, when a large enough area became suspended, it was energy-favourable for a small area close to the etch front to curl upward and the rest to curl downward. This effectively increased the height of etch channels at the etch front; hence, the transport speed of etchant and etching products prevailed against the speed of chemical reactions. The bilayers kept deforming when the SiO_2 sacrificial layer was attacked. Tubes were *instantly* formed when the last silicon oxide was removed from beneath. After 13.2 min of etching, 400 squares were completely curved into tubes (figure 2(c)). Figure 3 shows scanning-electron micrographs of tubes formed from different squares after etching under the same condition. All of the tubes had diameters of approximately $10.7 \mu\text{m}$ requiring a minimum side length of $10.7\pi/\sqrt{2} \mu\text{m} \approx 23.8 \mu\text{m}$ to form a complete tube. As shown in figure 3(a), where a curvature radius larger than $10.7/2 \mu\text{m}$ is observed⁶, $20^2 \mu\text{m}^2$ squares did not curl into tubes. Although the tubes were formed diagonally as shown in figure 3, the final orientation deviated from the square's-diagonal directions: for $30 \times 30 \mu\text{m}^2$ -sized squares about 62% tubes were left in the vertical direction, while 38% aligned with the horizontal direction (see figure 2(c)). The other array of squares on the same substrate showed a ratio of 55%:45%. In our experiment, the Reynolds number could be much lower than unity indicating that the inertial motion of the bilayers/tubes was overdamped⁷. However, partly due to the fact that the diagonals deviated from $\langle 010 \rangle$ by about $\pm 5^\circ$, *asymmetric* deformation of bilayers in such a viscous etchant liquid may result in a translational and/or rotational movement. The preference for tubes to form in the vertical direction is not yet fully understood. However, this preference of direction was not observed for those tubes with dimensions larger than the tube circumference ($33.6 \mu\text{m}$), instead more tube orientations were found because the squares had more degrees of freedom to deform when they were etched from all sides. With the benefit of a positive Poisson's ratio from the SiGe/Si medium, it is still possible to control the direction of curl by including asymmetric shapes in the initial pattern as starting points⁸. We found that the bilayer squares were strongly influenced by the surface tension of etchant liquid before they curled into tubes (see footnote 6). This relation was especially pronounced when there were bubbles forming on the bilayer surface and the bilayers could be distorted causing the etching to become non-uniform. With a larger number of turns, the tubes became stronger and less susceptible to surface tensions. After being dried in air, the tubes were found to have a strong adhesion to the substrate because of van der Waals forces between the SiGe layer and Si substrate.

⁶ These curved bilayers were flipped over by the fluidic current in cleaning processes after the etching. Curved bilayers have a smaller spring constant than complete tubes. Furthermore, they are not able to roll on the substrate as round complete tubes. When the solvent is evaporating, surface tensions bend the bilayers toward the substrate hence a larger curvature radius. Both curved bilayers and complete tubes are eventually held on the substrate by van der Waals forces.

⁷ Reynolds number is the ratio of inertial resistance to viscous resistance for a flowing fluid. In our current experimental setup, we are not able to measure the exact speed of fluid flow produced by curling bilayers. However, the lower bound of this speed is around $10 \mu\text{m s}^{-1}$, which corresponds to a low Reynolds number of approximately 10^{-3} . In this case, the viscous force dominates and the bilayers/tubes will hardly obtain any momentum from the shape deformation. However, an asymmetric deformation will result in a net displacement and/or rotation.

⁸ Poisson's ratio defines the coupling between the strains in two perpendicular directions. With positive Poisson's ratios, if a SiGe/Si bilayer curves downward in one direction, along the perpendicular direction it tends to curve upward.

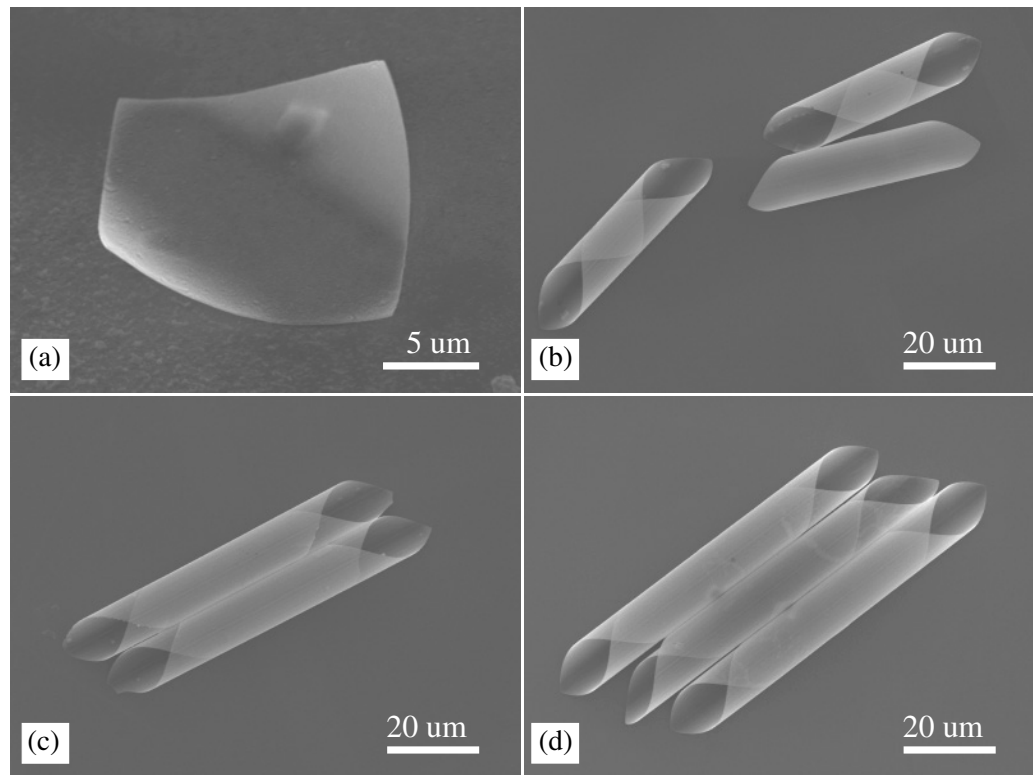


Figure 3. Scanning-electron micrographs of SiGe/Si tubes from (a) a $20^2 \mu\text{m}^2$ square, (b) three $45^2 \mu\text{m}^2$ squares, (c) two $60^2 \mu\text{m}^2$ squares, and (d) three $70^2 \mu\text{m}^2$ squares. The tube diameter is about $10.7 \mu\text{m}$.

Figure 4 shows the number of tubes formed as a function of etching time for different square sizes. For each curve, two distinct slopes are identified. Since bilayer squares curl into tubes only when they are completely suspended from the substrate, the smaller slope (which appears earlier than the larger slope) implies a higher mean etch rate. Furthermore, the smaller slope also indicates a larger deviation in etch rate. This high etch rate mode becomes dominant for squares larger than $45^2 \mu\text{m}^2$. Below $45^2 \mu\text{m}^2$, most of the tubes are formed in the low etch rate mode. A detailed evolutionary view of tube formation, as shown in figure 5, reveals that the etch rate is directly related to the degree of asymmetric surface deformation. Dynamic deformation of the bilayers as they were being suspended increased the height of etch channels from an initial value of 184 nm to approximately one on the order of $1 \mu\text{m}$. At the same time, etch channels were redirected. It is found that asymmetrically deformed bilayer squares had a much larger surface deformation than those which were symmetrically deformed. This peculiarity explains the large etching speed associated with asymmetric surface deformation. A slight irregularity arising from randomness in the chemical reactions and/or strain distributions can result in asymmetric etching with a high etch rate. It is also clear that the degree of freedom of those squares having asymmetric deformation became larger than that of the symmetrically deformed squares when their dimensions became much larger than the curvature radius. This diversity of deformed surface patterns results in a large deviation of the etch rate.

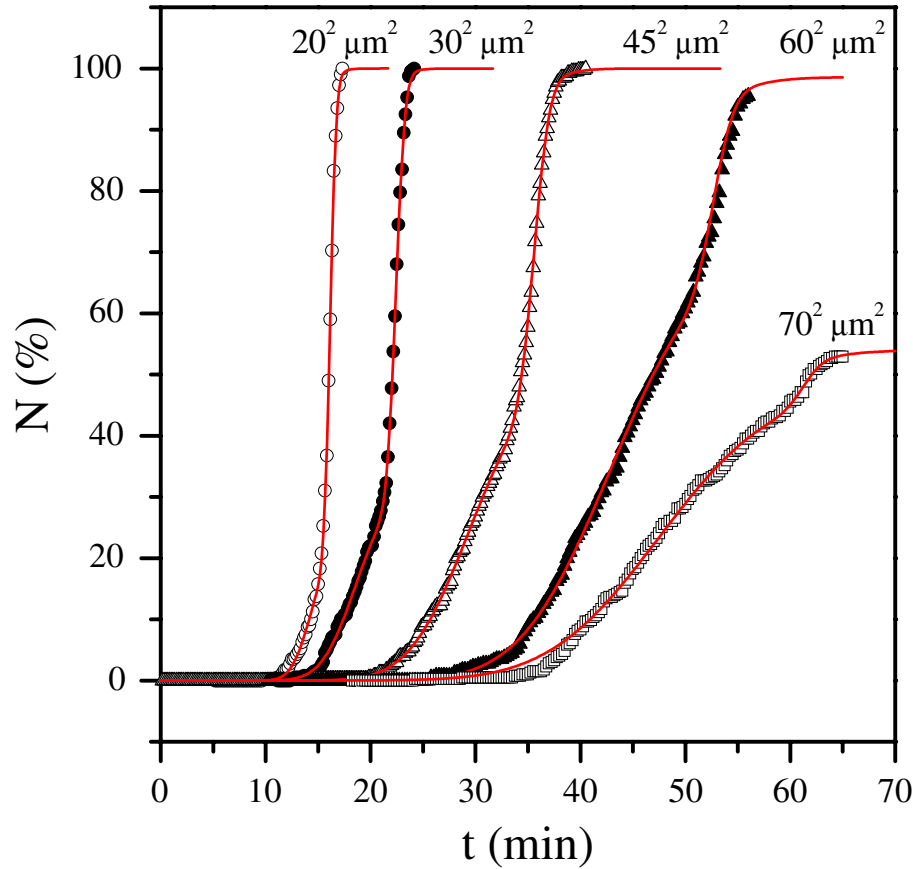


Figure 4. Tube formation as a function of etching time. Two different formation rates according to different slopes are identified. Solid curves are fits based on equation (1).

Assuming that the total etching time required to release a bilayer square from the substrate obeys a Gaussian distribution with a mean etching time T and a standard deviation σ , the tube formation curve follows

$$N(t) = N_1 \left[\frac{1}{2} + \frac{1}{2} \operatorname{erf} \left(\frac{t - T_1}{\sqrt{2}\sigma_1} \right) \right] + N_2 \left[\frac{1}{2} + \frac{1}{2} \operatorname{erf} \left(\frac{t - T_2}{\sqrt{2}\sigma_2} \right) \right]. \quad (1)$$

In this expression, N_1 and N_2 are the number of tubes formed in the fast and slow etching mode respectively and $\operatorname{erf}(x)$ is the error function. The solid curves based on equation (1) fit the experimental data shown in figure 4 very well. The mean etching times ($T_{1/2}$) and the standard deviations ($\sigma_{1/2}$) obtained from the above fitting procedure are presented in figure 6(a). When the chemical reaction at the etch front is strong enough so that there is a large gradient in the concentration of F^- and the reaction products ($(NH_4)_2SiF_6$ and H_2), the etching is transport-controlled. The mean etching time (T) of a parallel sacrificial layer as a function of the etched length (L) has the following relationship

$$T = A(e^{L/l_0} - 1), \quad (2)$$

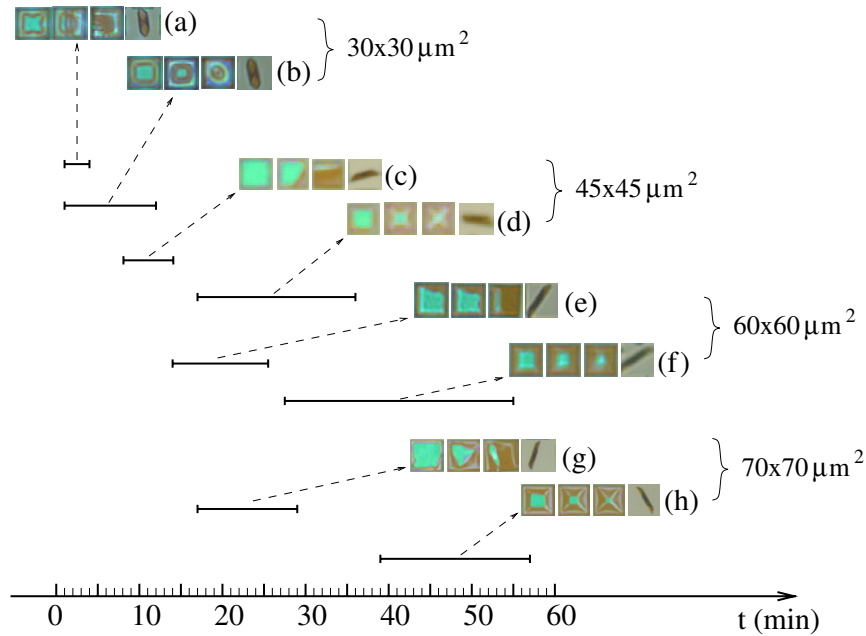


Figure 5. Snap shots show two different etching processes. Fast tube formation from a $30^2 \mu\text{m}^2$ square, a $45^2 \mu\text{m}^2$ square, a $60^2 \mu\text{m}^2$ square, and a $70^2 \mu\text{m}^2$ square are shown in (a), (c), (e), and (g), respectively. Correspondingly, much slower processes are shown in (b), (d), (f), and (h).

where both A and l_0 depend on the diffusion constants of F^- ions and reaction products, the reaction rate of F^- ions with the SiO_2 matrix and the concentration of F^- ions [15]. As shown in figure 6(a), T_1 has a linear dependence on the etched length L , which indicates that the diffusive transport of chemicals are fast enough such that the etching process is mainly determined by the chemical reaction at the etch front, namely a kinetic-controlled etching. Conversely, T_2 shows a nonlinear dependence on the dimension, indicating that transport-controlled etching processes do in fact exist. The dotted line in figure 6(a) is a fit of T_2 based on equation (2) with $A = 110.3 \text{ min}$ and $l_0 = 157.1 \mu\text{m}$. We believe that this observed T_2 is a mixture of both the transport-controlled and kinetic-controlled etching processes since the majority of the etch channels were kept in the transport-controlled mode when the surface was symmetrically deformed (see figures 5 (b), (d), (f), and (h)). On the contrary, asymmetric deformations induced a drastic changes in the etch channels causing the etching to become quasi-one-dimensional (see figures 5(a), (c), (e) and (g)). When the size of squares becomes sufficiently large, the degree of freedom in surface deformation becomes larger and the possibility for asymmetric etching increases, as shown in figure 6(b).

4. Conclusions

In conclusion, we have fabricated arrays of micrometre-sized SiGe/Si tubes by releasing the strain in the silicon layer using a SiO_2 -etching process. During the processing, bilayers strongly interacted with the etchant environment via chemical reactions and surface tension. The formation

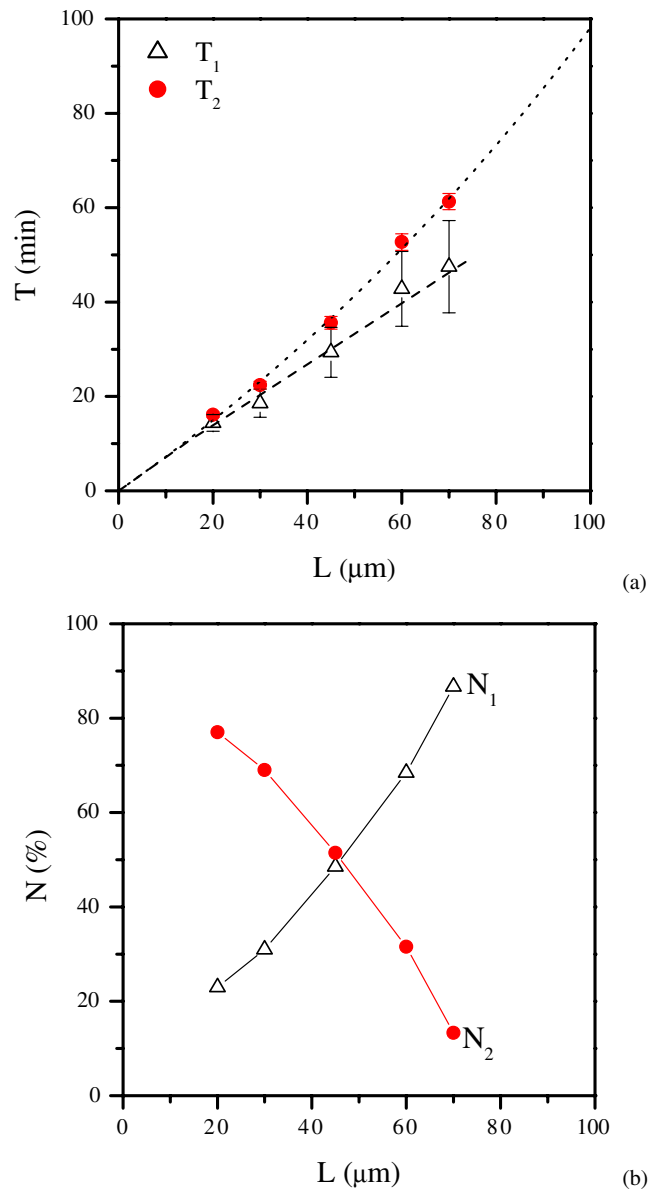


Figure 6. (a) Total etching time required to release the squares with different sizes. The solid circles are etching times required for the slow symmetric process. The dotted line is based on equation (2). The open triangles are for the fast asymmetric process. The dashed curve is a linear fit to those open triangles. (b) The percentages of tubes being symmetrically or asymmetrically etched as a function of square size.

dynamics strongly depended on the interplay of mechanical strain in the microstructure and the chemical reactivity. Once the bilayers were formed into tubes, they became less sensitive to the environment, e.g. humidity. However, van der Waals forces were strong enough to adhere the tubes at the silicon substrate. In the etching and curling processes, surface deformation due to the strain relaxation shifted the chemical etching from a transport-controlled mode to a

kinetic-controlled mode. These two modes are unique characteristics of separate etching processes. The slow etching process is associated with symmetric surface deformation and shows a nonlinear etch rate with a relatively little dispersion. The fast etching process is assisted by asymmetric surface deformation and shows a constant mean etching rate of about $1.5 \mu\text{m min}^{-1}$ with a larger dispersion of about $\pm 0.33 \mu\text{m min}^{-1}$. In the most common cases where the device is a few times larger than the curvature radius, the fast etching process with a large dispersion in etch rate becomes dominant. This study of the mechanism and dynamics of tube formation illuminates the necessity to meticulously control the etching process so that a uniform etch rate and a stable curling direction can be assured for releasing microtubes as ultra-sensitive sensors. As an outlook for future developments, the etch rate could be controlled in a more precise manner by employing an etch-stop process and incorporating a positive-Poisson's ratios by choosing a proper pattern design.

Acknowledgments

We would like to acknowledge funding through NIH (grant #2202636), a MRSEC/IRG1 seed grant (#DMR0079983) and AFRSO (#F49620-03-1-0420).

References

- [1] Nguyen C T-C 1999 *IEEE Trans. Microwave Theory Technol.* **47** 1486
- [2] Roukes M L 2001 *Phys. World* **14** 25
- [3] Huang X M H, Zorman C A, Mehregany M and Roukes M L 2003 *Nature (London)* **421** 496
- [4] Cleland A N and Roukes M L 1998 *Nature* **392** 160
- [5] Knobel R G and Cleland A N 2003 *Nature* **424** 291
- [6] LaHaye M D, Buu O, Camarota B and Schwab K C 2004 *Nature* **304** 74
- [7] Sazonova V, Yaish Y, Üstünel H, Roundy D, Arias T A and McEuen P L 2004 *Nature* **431** 284
- [8] Scheible D V and Blick R H 2004 *Appl. Phys. Lett.* **84** 4632
- [9] Prinz V Ya, Seleznev V A, Gutakovskiy A K, Chehovskiy A V, Preobrazhenskii V V, Putyato M A and Gavrilova T A 2000 *Physica E* **6** 828
- [10] Schmidt O G and Jin-Phillipp N Y 2001 *Appl. Phys. Lett.* **78** 3310
- [11] Vorob'ev A, Vaccaro P O, Kubota K, Aida T, Tokuda T, Hayashi T, Sakano Y, Ohta J and Nunoshita M 2003 *J. Phys. D: Appl. Phys.* **36** L67
- [12] *The International Technology Roadmap for Semiconductors (ITRS)* <http://www.itrs.net/>
- [13] Colinge J P 1997 *Silicon-on-Insulator Technology* 2nd edn (Dordrecht: Kluwer)
- [14] Voncken M M A J, Schermer J J, Bauhuis G J, van Niftrik A T J and Larsen P K 2004 *J. Phys.: Condens. Matter* **16** 3585
- [15] Monk D J, Soane D S and Howe R T 1993 *Thin Solid Films* **232** 1